A 'thermal fuse' in methionine biosynthesis arrests growth and protects *Escherichia coli* at elevated temperatures

Severin Schink[1,2,#,*], Zara Gough[2,#], Elena Biselli[2,#], Mariel Garcia Huiman[2], Yu-Fang Chang[1], Markus Basan[1], Ulrich Gerland[2,*]

[1] Department of Systems Biology, Harvard Medical School, 200 Longwood Ave, 02115 Boston, MA, USA

[2] Physics of Complex Biosystems, Physics Department, Technical University of Munich, 85748 Garching, Germany

[#]Contributed equally

*Corresponding authors: severin_schink@hms.harvard.edu and gerland@tum.de

Abstract

Microorganisms sense hazardous conditions and respond appropriately to maximize their survival. Adaptive stress resistance in microbes is mostly attributed to the expression of stress response genes, such as heat shock proteins, which prevent deterioration of cellular material. Here, we report a novel response of *E. coli* to heat stress: induction of a growth-arrested state, caused by degradation of an enzyme in the methionine biosynthesis pathway (MetA). We show that growth arrest has a direct benefit for survival at high temperatures; it protects cells when temperatures rise beyond 50ºC, increasing the survival chances by over 1000-fold. Using a combination of experiments and mathematical modelling, we show that degradation of MetA leads to the coexistence of growing and non-growing cells, allowing microbes to bet-hedge between continued growth if conditions remain bearable and survival if conditions worsen. We test our model experimentally and verify quantitatively how protein expression, degradation rates and environmental stresses affect the partitioning between growing and non-growing cells. Because growth arrest can be abolished with simple mutations, such as point mutations of MetA and knock-outs of proteases, we interpret the breakdown of methionine synthesis as a system that has evolved to disintegrate at high temperature and shut off growth, analogous to 'thermal fuses' used in engineering to shut off electricity when the device could be damaged by overheating.

35 **Introduction**

36 Bacteria in nature face a variety of environments, ranging from ideal growth
37 conditions to hostile environments, where stressors threaten the survival of the
38 population. One such stressor is elevated temperature, which can arise quickly
39 and unpredictably. In order to survive when temperatures rise above the optimal
40 range, bacteria employ a well characterized heat shock response [1–3] that aims at
41 maintaining the functionality of the cell. Molecular chaperones protect proteins in
42 the cytoplasm and periplasm by maintaining their native conformation [4,1,2] and
43 proteases degrade misfolded and aggregated proteins [5]. DNA repair is upregulated
44 [6] and toxic reactive oxygen species, which are at particularly high levels at
45 elevated temperatures [7], are scavenged by catalases [8], superoxide dismutases [9],
46 and small molecules like glutathione [10]. The induction of these protective genes,
47 collectively referred to as the heat shock response, allows bacteria to maintain
48 their functionality and recover once conditions have improved.

49

50 Here, we report an orthogonal response to heat stress, that is not based on the
51 expression of stress response genes, but instead on the degradation of a key
52 enzyme, causing cells to stop growing. Growth arrest seems counter-intuitive as
53 an active response to stress, because growth arrest in conditions that still support
54 growth is a fitness defect, but it is frequently encountered in a variety of microbes
55 across the phylogenetic spectrum [11] when exposed to stress conditions outside of
56 the optimal culture conditions [12,13,11]. A growing body of literature suggests the
57 importance of growth arrest in the context of 'viable but not culturable' (VBNC)
58 states[11,13] and persistence[14,15], in particular in food safety[16,17] and antibiotic
59 treatment[14]. However, pinning down mechanisms of how bacteria achieve growth

60 arrest and why such mechanisms have evolved has proven challenging [18,19], which
61 stands in the way of positively identifying growth arrest as an evolved strategy.
62
63 In this work, we describe heat-induced growth arrest in *Escherichia coli*, and show
64 that the growth-arrested state protects from cell death when temperature is
65 further increased. This protective effect of growth arrest against heat shocks
66 appears to be a more general physiological feature of microbes, as we can
67 reproduce the phenomenon in *Saccharomyces cerevisiae*. For *E. coli,* we elucidate
68 the molecular mechanism underlying heat-induced growth arrest using a
69 combination of quantitative experiments and theory. We show that *E. coli* can
70 control how many cells in a population become growth-arrested, and thus
71 protected from heat shocks, through active degradation of the enzyme MetA.
72 Taken together, this establishes self-controlled growth arrest in microbes as a
73 physiological strategy to combat heat stress.

74 **RESULTS**

75 *Elevated temperatures induce growth arrest in E. coli*

76 To probe how heat affects the physiology of bacteria, we exposed cultures of
77 *Escherichia coli* K-12 grown in minimal medium at elevated temperatures to a
78 period of carbon starvation. During this period, the absence of *de novo* synthesis
79 reveals the deteriorative effects of temperature on the cell. After the starvation
80 period, we reinoculated the culture in fresh medium with a carbon substrate and
81 observed the resulting recovery of the stressed culture. The temperature was kept
82 constant throughout the entire experiment, i.e. initial growth, starvation, and
83 recovery. We observed that the regrowth during the recovery phase displays lag
84 times that depend on temperature (Fig. 1A). At 37ºC, cultures recovered quickly,
85 while at 45ºC, the maximum growth temperature, the culture required more than
86 10 h to recover. Such long recovery times at high temperatures are puzzling,
87 because the majority of bacteria were still viable at the time of reinoculation, as
88 assayed by plating on LB agar at 37ºC (Fig. S1), implying that the long lag times
89 are not due to cell death, but instead caused by viable bacteria not growing.

90

91 The lag time also increases with the prior starvation duration (Fig. 1B), suggesting
92 that cells gradually lose the ability to grow. For 1 hour of starvation, cultures
93 recovered within 2 hours, but if starvation took longer than 9 h at 45ºC, cultures
94 did not recover within the 3 days of the experiment.

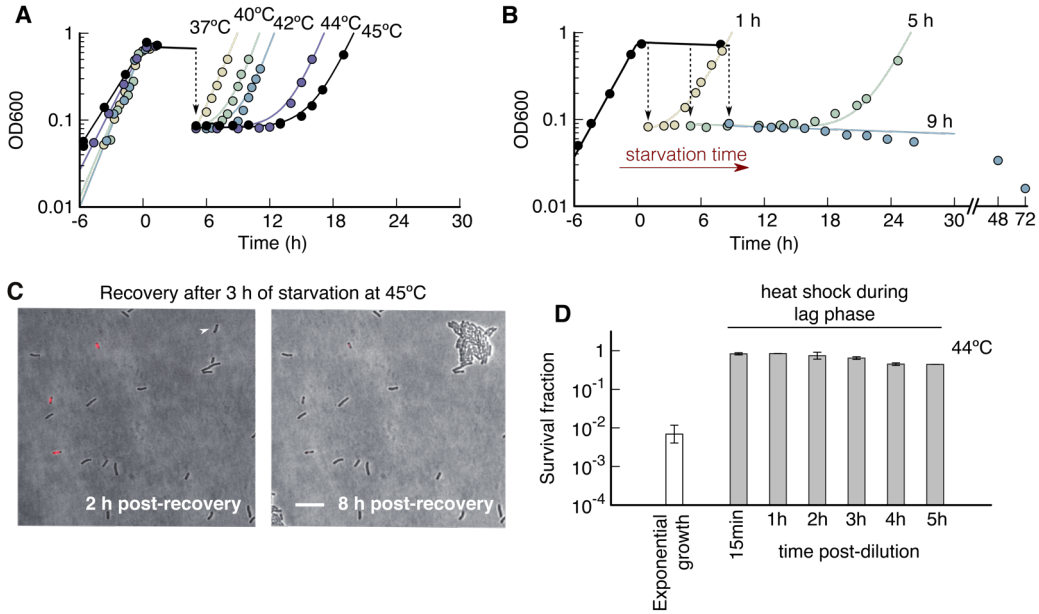

Figure 1 ***Growth arrest at high temperatures protects Escherichia coli in heat shocks. (A)*** *Optical density OD_{600} of Escherichia coli K-12 grown until nutrient depletion, first starved for 5 hours, then diluted into fresh medium to allow recovery. Colors denote culture temperatures, kept constant throughout each experiment. Lag times of cultures increase with temperature, from ~23 min at 37 °C, to 11.1 h at 45 °C. In panels A-C, growth is fitted as exponential $N(t) = N(0)e^{\mu t}$ and recovery as a combination of decay and growth $N(t) = N_1 e^{-\gamma t} + N_2 e^{\mu t}$, with $\gamma = 0.1\ h^{-1}$. Lag times are extracted as detailed in Methods.* ***(B)*** *Lag times at 45ºC increase with starvation duration. No recovery was recorded within 3 days for 9 h starvation (blue) or longer.* ***(C)*** *Snapshots of time-lapse movies during recovery at 45 °C on glycerol minimal medium agar pads, see Methods. Fluorescence of propidium iodide (red) reports permeability. One growing cell (white arrow) grows to a microcolony after 8 h of incubation. Scale bar: 10 µm. (**D**) Killing by heat shock (52ºC, 10min) of E. coli cultured at 44ºC in exponential growth (white) or during lag phase after 3 h of starvation and dilution (grey). E. coli growth arrested during lag phase are completely protected from heat killing at 52ºC.*

There are two qualitatively different scenarios for how long lag times can arise. One scenario is a homogeneous population of cells that all require a similarly long time to recover. The other scenario has two subpopulations, a large non-growing population and a small growing population. In the second case, the lag time is given by the time it takes for the small, growing population to dominate the cell count. To distinguish between these scenarios, we assayed the recovery phase at the single cell level: we extracted samples of a starved culture at 45ºC and deposited them on pre-warmed agar pads supplemented with carbon substrate to

104 allow recovery. We stained the bacteria with propidium iodide (red) for
105 membrane permeability to detect cell death, and monitored growth by time-lapse
106 microscopy (see Methods). Figure 1C shows two snapshots from a time-lapse, 2 h
107 and 8 h after nutrient addition: The culture, previously starved for 3 h, shows
108 three distinct populations. 5% of the population stains positive for cell
109 permeability and are likely dead. A second, small subpopulation, 2%, recovered
110 after about 2 hours, and after 8 h has formed micro-colonies, which are visible in
111 Figure 1C (white arrow). The third and major subpopulation, 93%, stained
112 negative for cell permeability, but did not grow within the 12 h of this time lapse.
113 This data shows that recovery is highly heterogeneous; few cells recover early and
114 dominate the recovery.
115
116 In an experimental scenario similar to ours, Trip & Youk recently observed that
117 *Saccharomyces cerevisiae* arrest growth when cultures are diluted during
118 exponential growth at elevated temperatures[20]. Indeed, this density-dependent
119 growth behavior is shared by *E. coli*: we found that if cultures are diluted during
120 exponential growth, they also enter growth arrest (Fig. S5A). This poses an
121 interesting possibility that heat-induced growth arrest is a more general hallmark
122 of microbes, and triggers the question: Is there a fitness benefit to heat-induced
123 growth arrest ?
124
125 *Growth-arrest protects E. coli from heat shocks*
126 Because growth arrest is unique to temperatures close to the growth limit (40-
127 45ºC for *E. coli)*, but in a regime where conditions still allow growth, we wondered
128 if growth arrest is an evolutionarily 'chosen' strategy, rather than an accident. For

129 such a strategy to evolve, there would need to be a selective benefit associated
130 with growth arrest, which outweighs the cost of reduced growth. To examine
131 possible selective benefits, we exposed *E. coli* cultures to sudden heat shocks. We
132 used our standard starvation protocol (Fig. 1A-C) to induce growth arrest, using a
133 5h period of starvation and subsequent reinoculation in fresh medium at 44ºC. We
134 took samples from the culture every hour after reinoculation, heat shocked them
135 for 10 min at 52ºC, and measured the resulting viability. Strikingly, growth-
136 arrested cultures survived heat shocks almost unscathed, while in cultures heat
137 shocked in exponential growth, only about 0.7% survived (Fig. 1D). The existence
138 of this benefit shows that growth arrest could in principle be used by
139 microorganisms as a part of the response to heat stress. To investigate this
140 possibilty, we next sought to understand what causes *E. coli* to enter growth
141 arrest.
142

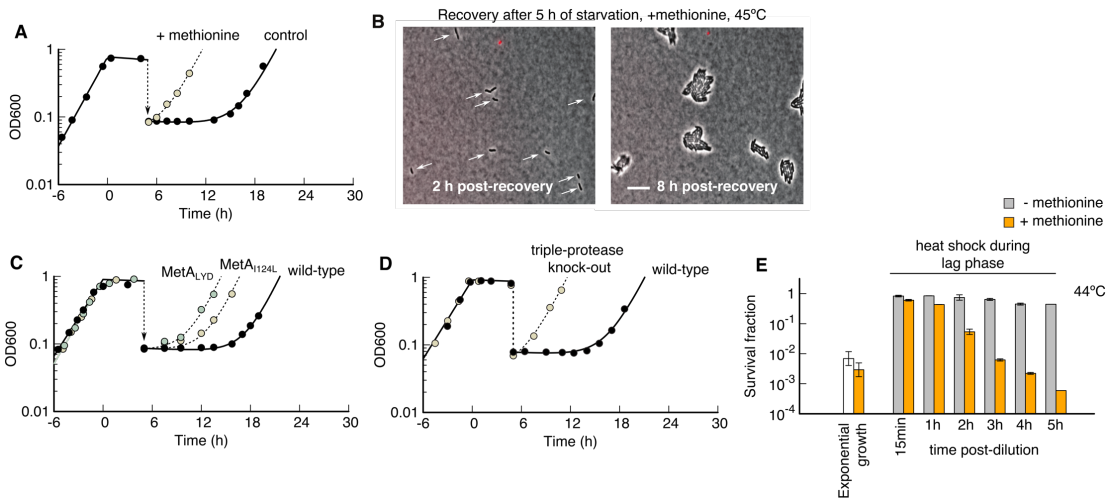

Figure 2 ***Growth arrested cells are methionine limited due to MetA degradation. (A)*** *Cultures supplemented with methionine recover quickly. Lag times (45ºC, 5 h starvation) in cultures supplemented with methionine during the entire experiment are more than 90% shorter than without methionine ($T_{lag} = (0.64 \pm 0.02)$ h compared to $T_{lag} = (11.08 \pm 0.4)$ h, N = 2, p < 0.001). (**B**) Snapshots of a time-lapse of recovery on glycerol agar pads supplemented with methionine. Cells indicated with white arrows recover and form microcolonies after 8 hours. Scale bar: 10µm. (**C**) Comparison of wild-type MetA with two thermostable mutants. Lag times (45ºC, 5 h starvation) decrease in mutants MetA I124Y ($T_{lag} = (5.2 \pm 1.0)$ h, N = 3, p < 0.001) and LYD ($T_{lag} = (3.7 \pm 0.9)$ h, N = 3, p < 0.001) compared to wild-type ($T_{lag} = (11.1 \pm 0.3)$ h, N = 3). (**D**) Comparison of wild-type E. coli with a triple protease knock-out (Δlon, ΔhslV & ΔclpP). Absence of protease activity decreases lag time ($T_{lag} = (1.1 \pm 0.3)$ h, N = 3, p = 0.0012) compared to wild-type ($T_{lag} = (10.4 \pm 1.6)$ h, N = 3). (**E**) Heat shocks (10 min at 52ºC) during exponential growth and during lag times at 44ºC in cultures supplemented with and without methionine. Killing of the methionine-supplemented culture coincides with growth (at 2h: 2-fold increase of CFU/ml, at 5h: 20-fold increase of CFU/ml).*

Breakdown of methionine synthesis causes growth arrest in E. coli

It is known that high temperature leads to denaturation of the proteome [21,22]. One protein, homoserine O-succinyltransferase (MetA), which catalyzes the first commitment step of the methionine biosynthesis pathway, is particularly susceptible to heat stress [23–25]. This enzyme aggregates and is degraded [26]. To test if the long lag times are due to methionine limitation, we supplemented the medium with methionine and found a drastic reduction in lag time, from over 10 hours without methionine, down to less than 30 minutes with methionine (Fig. 2A). Similarly, growth arrest induced by dilution was also alleviated by the presence of methionine, decreasing the minimum initial population density from

153 which cultures could regrow 100-fold (Fig S5). Investigating lag times on a single-
154 cell level, we found that if the agar pad is supplemented with methionine, the
155 majority of the cells recovered after starvation (63% compared to 2% w/o
156 methionine), while the growth-arrested and non-permeable subpopulation
157 virtually disappeared (5% compared to 93% w/o methionine), see Figure 2B. The
158 absence of the growth-arrested subpopoulation (Fig. 2B) is consistent with the
159 drastic reduction in lag times observed in bulk measurements (Fig. 2A).
160
161 To test if methionine limitation is due to MetA degradation, and not a different
162 enzyme in the methionine pathway, we tested MetA mutants with reduced
163 degradation rates, either due to a single point mutation (I124L) or three point
164 mutations (I124L-I229Y-N267D – abbr. LYD) identified by Mordukhova and
165 coworkers [27]. Indeed, these mutants, which have 2-3 fold decreased degradation
166 rates [27], showed a significant decrease in lag times from about 11 h to about 5 h
167 for the single point mutant (I124L) and 4 h for the triple-point mutant (LYD) (Fig.
168 2C).
169
170 When we hypothesize growth arrest to be a response to heat stress, an important
171 question is whether MetA is degraded because it is broken, e.g. aggregated or
172 otherwise damaged, or whether MetA is degraded despite being still functional.
173 The latter option would speak for growth arrest being a 'self-inflicted injury',
174 rather than an accident. To distinguish these two possibilities, we constructed a
175 triple knock-out of proteases Δ*lon, ΔhslV* and Δ*clpP,* incapable of degrading
176 cytoplasmic proteins, in particular MetA[25]. If MetA is broken, lag times should
177 either remain unchanged or increase in this triple protease knock-out mutant. On

178 the other hand, if functional MetA is actively degraded in wild-type, lag times will
179 decrease in the mutant. In the experiment, we found a striking decrease of lag time
180 from 10 h in wild-type down to 1 h in the triple protease knock-out (Fig. 2D),
181 strongly suggesting that methionine limitation is caused by degradation of
182 *functional* MetA. This implies that the methionine limitation is brought upon the
183 cell by itself, rather than being caused exclusively by stressors.
184
185 If growth arrest protects *E. coli* during heat shocks, and growth arrest is in turn
186 due to methionine limitation, then the addition of methionine should render cells
187 susceptible to heat again. We tested this hypothesis on cultures that were grown,
188 starved, and reinoculated at 44˚C in media with and without methionine, and then
189 heat-shocked at 52˚C (see `Methods'). While cultures without methionine were
190 protected for several hours from heat, cultures with methionine lost more than
191 99.9% of their viability soon after reinoculation in fresh medium (Fig. 2E).
192
193 *Metabolic bistability leads to stable growth arrest*
194 How does methionine limitation trap cells in a state of growth arrest? This is
195 particularly important in order to understand which mechanisms microbes could
196 use to manipulate the fraction of cells entering growth arrest depending on
197 external conditions. While it is clear that degradation of MetA is detrimental for
198 growth, it is important to note how stable growth arrest is: entire cultures can
199 remain growth-arrested for several days, although the conditions would allow for
200 growth in principle (Fig. 1). This stability of growth arrest is puzzling because one
201 would expect that any residual amount of MetA activity, or import of methionine
202 from perished cells, would kickstart growth by supplying methionine, which in

203 turn will be used to synthesize MetA in a self-enhancing positive feedback loop. To
204 answer these questions, we designed a mathematical model of metabolism and
205 protein synthesis that describes the dynamics of internal methionine
206 concentration c_{met} and MetA abundance ϕ_{MetA}. We will use the model to derive a
207 theoretical prediction of lag time, and to perform quantitative tests of our
208 hypotheses.
209
210 The model, summarized in Fig. 3A, incorporates processes that affect the cellular
211 methionine level (solid lines) and the MetA protein abundance (dashed lines).
212 Within this model, growth is limited by methionine, Eq. (1), and MetA is degraded
213 at rate γ, diluted by growth and synthesized together with biomass at rate μ, Eq.
214 (2). Methionine can either be produced by MetA, or taken up from the
215 environment, and is used for protein synthesis and to synthesize S-adenosyl-
216 methionine (SAM), the major methyl donor of the cell, Eq. (3). While much of this
217 SAM is recycled back to methionine in the SAM cycle (Fig. S3), a significant part is
218 used for biosynthesis of polyamines (Table S2), such as spermine and spermidine,
219 which are important for survival in stress conditions [28–30]. We account for SAM
220 synthesis and other potential losses of methionine flux in a drainage flux (Fig. 3A).
221 In the Supplementary Information we show a detailed derivation of the model and
222 in Table S2 we estimate model parameters based on published measurements.

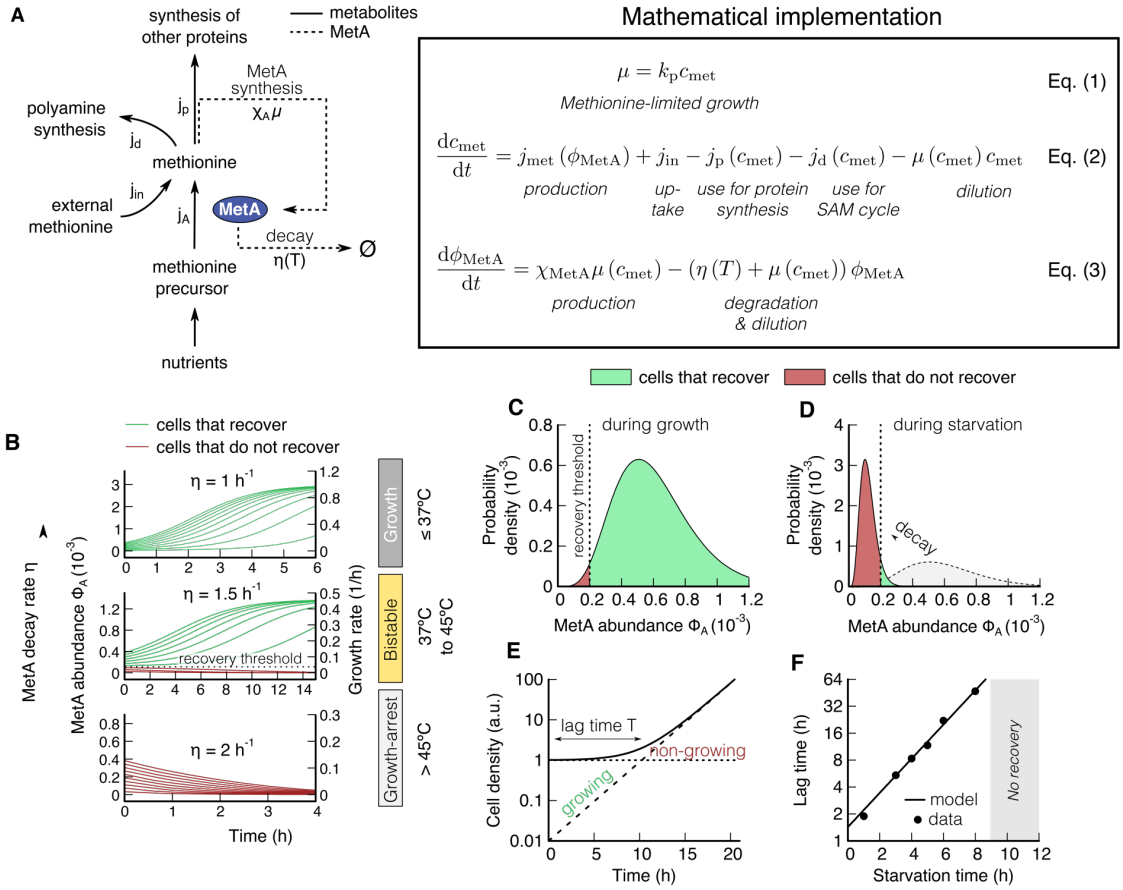

Figure 3 ***Methionine-MetA model shows that bistability arises from dual use of methionine.*** *(**A**) Cartoon of the methionine-MetA model. Metabolites: nutrients are taken up, converted first to precursors and finally to methionine by MetA (pink). See Figure S3 for a detailed methionine biosynthesis pathway. External methionine can be imported, if present in the medium. Two fluxes drain methionine, protein synthesis and polyamine synthesis. Proteins: MetA (pink) is synthesized if methionine is present, and will in turn synthesize methionine (positive feedback loop). MetA is degraded at a temperature dependent rate.* ***(B)*** *Numerical results of the dynamics of the methionine-MetA model for three different MetA degradation rates (1.0/h, 1.5/h and 2/h). Whether cells can recover depends on the temperature dependent degradation rate. At intermediate temperatures (middle), we observe that only cells with an initial MetA abundance above a recovery threshold can recover (bistable regime).* ***(C-D)*** *Distribution of MetA abundance during growth and starvation. Green and red areas indicate cells with MetA abundance that allow (green) and do not allow (red) growth.* ***(E)*** *Recovery dynamics of a mixed culture in batch. The time it takes for the growing fraction to overgrow the non-growing fraction is the lag time.* ***(F)*** *Theoretical prediction of lag times compared with experiments (45ºC). Lag time increases exponentially with starvation time* $T_{lag} = (1.6 \pm 0.3)\, exp(\tau\, (0.43 \pm 0.02)\, h^{-1})$*. When cultures are starved for more than 9 hours, they do not recover within three days. The exponential rate fitted,* $\eta = 0.46\, h^{-1}$*, is lower than the in-vitro MetA decay rate* $1.6\, h^{-1}$ *measured in Ref.* [27]*, possibly due to low levels of ATP that is required for active degradation during starvation* [25]*.*

The recovery dynamics of the methionine-MetA model depends on the degradation rate of MetA (Fig. 3B): At low degradation rate, all cells, regardless of their initial state, recover to growth (top panel, green trajectories), while at high

227 degradation rate, none of the cells recover (bottom panel, red trajectories). In
228 between these two extremes, the population splits depending on the initial MetA
229 abundance (Fig. 3B, middle). Cells above a certain 'recovery threshold' accumulate
230 MetA and start growing, while cells below the threshold do not. Because both
231 growth and growth-arrest are stable states, this intermediate regime is bistable,
232 and a population can contain cells that are growing and others that are not.
233 Because of the positive-feedback motif between methionine and MetA, the
234 bistability requires a non-linearity in flux[31], which in our model is caused by the
235 drain of methionine to SAM and disappears if either the drain is shut off (Fig. S4A)
236 or if methionine is supplemented in the medium (Fig. S4B).
237
238 Because whether an individual cell recovers or stays dormant depends on its
239 initial MetA abundance, we suspect that fluctuations in MetA abundance cause the
240 split of the population. Protein abundance is indeed highly variable among
241 individual bacteria due to the stochasticity of transcription and translation
242 processes[32,33], with a typical standard deviation of 40% [33]. We thus hypothesize
243 that during growth, the vast majority of cells will lie above the recovery threshold
244 (Fig. 3C), and that only due to starvation at elevated temperatures, where MetA
245 will be degraded but not synthesized, the abundance distribution will shift to
246 lower values and many cells will fall below the threshold (Fig. 3D). As a result, only
247 the exponential tail of the MetA abundance distribution will remain above the
248 recovery threshold, leading to a small population of recovering cells. According to
249 the model, the characteristic long lag times observed in Fig. 1 emerge from this
250 mixture of growing and non-growing cells (Fig. 3E).
251

252 The model predicts (Supplementary Text 1C) how lag time depends on the
253 fraction of recovering cells, and how degradation of MetA reduces the fraction of
254 recovering cells. We find a simple exponential dependence between lag time T_{lag}
255 and the starvation time τ and degradation rate η,

$$T_{\mathrm{lag}} \propto \bar{\phi}_{\mathrm{MetA}}^{-1} \exp(\eta\tau)\,, \qquad (1)$$

256 which originates from the exponential tail of MetA abundance, caused by the
257 stochasticity of transcription and translation processes ($\bar{\phi}_{\mathrm{MetA}}$ denotes the mean
258 MetA abundance).
259
260 A key prediction from the model in Eq. (4) is that the lag time T_{lag} should increase
261 exponentially with starvation time τ. Because lag time in the model is set by the
262 fraction of the population that recovers, this dependence gives us a direct test of
263 what determines how many cells get trapped in the growth arrest state. Indeed,
264 we can verify the exponential scaling law, and find that it holds over a striking 50-
265 fold range in lag times (Fig. 3F). Cultures starved for more than 9 hours did not
266 recover within 3 days, presumably because all cells of the population are trapped
267 in the growth-arrested state.
268
269 The MetA mutants with reduced degradation rates give us the opportunity to test
270 how evolution can tune the fraction of growth-arrested cells, and hence the lag
271 time. The single point mutant I124L, has an experimentally measured degradation

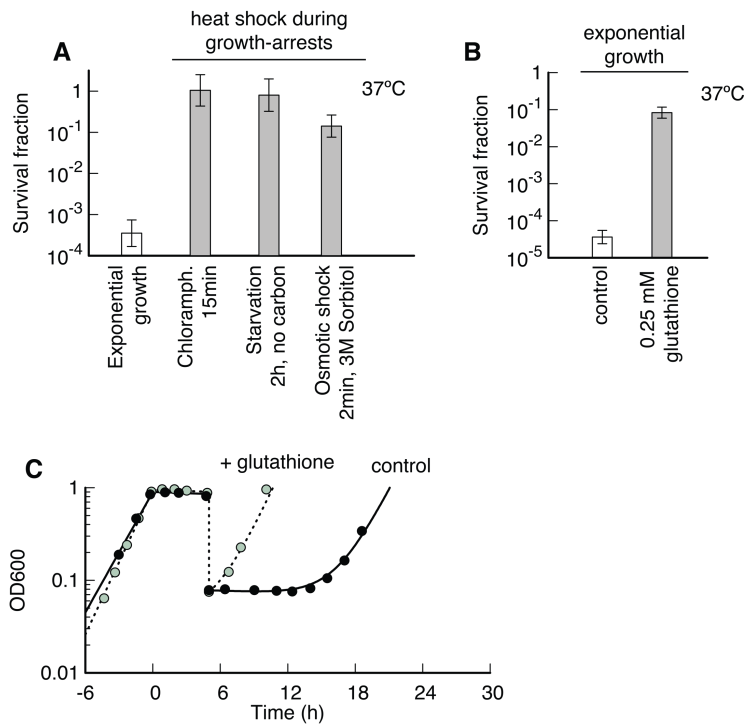

Figure 4 ***Oxidative stress at elevated temperatures****. (**A**) Killing by heat shock (50ºC, 10min) of E. coli cultured at 37ºC either in exponential growth (white) or in growth arrest caused by translation inhibition (chloramphenicol), carbon starvation or hyperosmotic shock (grey). Protection from heat killing is independent of the cause of growth arrest. (**B**) Addition of the antioxidant glutathione rescues heat-induced death (50ºC, 10 min) in exponential growth indicating that oxidative damage is involved at heat-induced death. (**C**) Addition of glutathione reduces lag times after 5h of starvation from ($T_{lag} = (1.4 \pm 0.2)$ h to $T_{lag} = (10.3 \pm 1.6)$ h, N = 3, p = 0.0013).*

rate reduced by 48% compared to wild-type[27]. Using the fit from Fig. 3F, we predict that this mutant should display a lag time of $T_{\mathrm{lag}} = (4.5 \pm 1.0)$ h, which matches the observed (5.2 $\pm$ 1.0) h of Fig. 2C well.

Growth arrest protects cells irrespective of cause

Finally, it is still unclear how heat-induced growth arrest protects cells from subsequent heat-shocks. One possibility is that heat shock proteins, expressed during growth arrest, prepare cells for the upcoming heat shock. To test this hypothesis, we blocked translation during exponential growth by adding chloramphenicol, which leads to growth arrest without new proteins being synthesized [34]. These experiments were performed at 37ºC, where cells are particularly susceptible to subsequent heat shocks. Remarkably, cultures arrested

284 with chloramphenicol survived heat shocks without a significant decrease in
285 viability, whereas the viability of untreated cultures in exponential growth
286 decreased by more than 99.9% (Fig. 4A). Growth arrest by inhibition of protein
287 synthesis thus phenocopies the effect of methionine-limited growth arrest (Fig.
288 2E). Two alternative types of growth arrest, hyperosmotic shock (3M sorbitol) and
289 sudden carbon starvation (culture washed during exponential growth and
290 resuspended in carbon-free medium, then starved for 2 h, thus preventing
291 adaptation during the stationary phase), also yielded similar protection from heat
292 shocks (Fig. 4A), suggesting that growth arrest by itself, independent of the
293 underlying cause, is protective.
294
295 *Oxidative damage contributes to heat-induced death*
296 What are growth-arrested bacteria protected from? For eukaryotic microbes like
297 *Saccharomyces cerevisiae* [35,36] and animals like gold fish [37,38] it was shown that
298 oxidative damage is involved in heat-induced stress and death. To reduce
299 oxidative damage at high temperatures, *S. cerevisiae* exports antioxidants such as
300 glutathionine [20]. For bacteria, a similar connection between oxidative stress and
301 temperature stress was hypothesized, based on the observation that temperature
302 sensitive mutants are hypersensitive to oxidative stress [39]. To test if oxidative
303 stress is indeed involved in heat-induced death, we supplemented cultures in
304 exponential growth at 37ºC with glutathione and performed heat shocks.
305 Strikingly, we found that glutathione-supplemented cultures in exponential
306 growth survive 1000-fold better compared to an untreated control (Fig. 4B). This
307 result indicates that growth arrest alleviates lethal oxidative damage that would
308 otherwise kill in heat shocks.

309

310 Because oxidative damage is well known to induce aggregation[40,41] and
311 proteolysis [42,43], akin to the aggregation and degradation observed for MetA at
312 high temperatures [25,26], we tested if adding the antioxidant glutathione in our
313 standard starvation and reinoculation protocol influences lag times. We found a
314 drastic reduction in lag times for cultures supplemented with glutathione, from
315 10.4 h to 1.4 h (Fig. 4C). Because lag times are caused by degradation of MetA (Fig.
316 2), this result suggests that oxidative damage is the trigger for MetA degradation.
317 Similarly, glutathione prevents growth arrest at elevated temperatures in yeast [20],
318 suggesting that oxidative damage causes growth arrest more generally in
319 microbes. To test if growth arrest in yeast is also caused by methionine limitation
320 or by a different mechanism, we tested if growth arrest of *Sacharomyces cerevisiae*
321 at 39ºC can be rescued with methionine. We found no difference in growth
322 between methionine-supplemented cultures and controls (Fig. S6 A-B), showing
323 that for yeast, growth arrest is caused by a different mechanism. The protective
324 feature of growth arrest, however, is shared by yeast: While growing yeast (30ºC)
325 died by a factor of 500 during heat shocks, starving yeast largly survived (Fig S6
326 C). Taken together, these findings show that employing growth arrest to combat
327 heat-induced death may be a more general strategy of microbes.

328 **DISCUSSION**

329 We have shown that breakdown of methionine biosynthesis at elevated
330 temperatures causes growth arrest in *Escherichia coli*. Despite its fitness cost
331 under habitable conditions, growth arrest is beneficial for *E. coli* because it
332 protects cells from heat-induced death when temperatures rise beyond 50ºC. We
333 demonstrated that this growth arrest can be alleviated by simple point mutations
334 and knock-outs. We therefore suggest that it constitutes a self-controlled growth
335 arrest that has likely evolved as an active response to heat stress, orthogonal to
336 the well-studied heat shock response.

337

338 *Shut-off of methionine synthesis is ideally suited to halt growth*

339 While a lack of any amino acid would stop translation, lack of methionine
340 specifically halts translation initiation, because the majority of bacterial start
341 codons code for N-formylmethionine (fMet), a direct derivative of methionine.
342 Lack of other amino acids would halt elongation after initiation, leading to protein
343 fragments that would need to be recycled by the cell. Furthermore, inhibition of
344 translation triggers the stringent response alarmone (p)ppGpp [44]. This global
345 regulator in bacteria inhibits synthesis of rRNA and tRNA [45], transcription [46], as
346 well as DNA replication [47,48], leading to a global shut-off in macromolecule
347 synthesis. At the same time, the central metabolism and generation of energy-rich
348 molecules are upstream of MetA, so that cells are presumably well fueled to
349 perform energy-dependent maintenance. This combination of inhibited
350 biosynthesis, but non-inhibited metabolism makes methionine an ideal bottleneck
351 to induce growth-arrest in bacteria, which lack global regulators of growth, such
352 as mTOR.

353

354 *MetA is a biological 'thermal fuse'*

355 The temperature-induced degradation of MetA has a counterpart in electrical
356 engineering: electrical devices are protected from excessive heat with 'thermal
357 fuses', which cut off electric current by physically disintegrating, typically by
358 melting. The fuse has the role of an emergency protection, kicking in when other
359 regulatory mechanisms have failed, in order to protect expensive components. In
360 a similar manner, we interpret MetA as a biological thermal fuse. If the benefit of
361 increasing survival chances outweighs the cost of increased synthesis and missed
362 potential for growth, then the thermal fuse will have a net positive effect on fitness.
363 The high expression levels combined with high degradation rates, as we observe
364 in the case of MetA, reflect a highly volatile strategy, typical for biological
365 regulators [49]. In fact, it is ideally suited to stressful conditions to ensure fast
366 growth if conditions are bearable, while also quickly shutting off biosynthesis if
367 conditions worsen.

368

369 *Bet-hedging between growth and survival in anticipation of rare catastrophic events*

370 The bistability in growth arrest could play a vital role in optimizing fitness at
371 elevated temperatures. Because both growth and growth arrest are stable, the
372 bacterial population can split into two subpopulations. If individual cells can
373 switch between states of growth and arrest depending on the external
374 environment and their internal methionine concentration, then according to the
375 model, the fitness of the population is optimized by partitioning the population
376 into two sub-populations; a growing and growth-arrested population. Such a
377 mixture of two distinct behaviors in a genetically homogeneous population of cells

is a hallmark of bet-hedging strategies, typical for biolgical systems in unpredictable environments [50–52]. Bet-hedging aims to increase long-term fitness beyond what would be possible for either pure strategies of growth and growth arrest. Thus having a growth-arrested subpopulation will allow microbes to survive sudden heat shocks, while at the same time proliferating at sub-critical temperatures – enabling them to robustly thrive at the edge of habitable conditions.

Acknowledgments

This work was supported by the German Research Foundation (DFG) via the Excellence Cluster ORIGINS (through U.G.), and by the Life initiative of the Volkswagen Foundation (through U.G.). E.B. was supported by a DFG fellowship through the Graduate School of Quantitative Biosciences Munich (QBM). S.J.S was supported by a Long-Term Fellowship (ALTF 782-2017) from the European Molecular Biology Organization (EMBO) and Long-Term Fellowship (LT000597/2018-L) from the Human Frontiers in Science Program (HFSP).

Author contributions

SJS and UG conceived this study. SJS, EB, MGH and ZG designed and performed experiments. YFC constructed strains. SJS, MB and UG developd the theoretical model. SJS, EB, MB and UG wrote the paper. MB and UG funded and supervised the project.

Data availability statement

Source data of figures are available upon request from the corresponding authors.

Code availability

The numerical implementation of the theoretical model used to generate Figure 3 is available upon request from the coresponding authors.

Declaration of interests

The authors declare no competing financial interests.

410 **METHODS**

411 *Contact for Reagent and Resource Sharing*

412 Further information and requests for resources and reagents should be directed
413 to and will be fulfilled by the lead contact.

414

415 *Strains*

416 All strains used in this study are derived from wild type *E. coli* K-12 strain
417 NCM3722 [53]. Amino acid substitutions $MetA_{I229Y}$ and $MetA_{LYD}$ (containing point
418 mutations I124L-I229Y-N267D) in strains I229Y and LYD [27] were transferred to
419 NCM3722 ΔMetA via P1 transduction to yield strains YCE55 (NCM3722 $metA_{I229Y}$)
420 and YCE57 (NCM3722 $metA_{LYD}$), using methionine as a selective marker.

421

422 *Culture media*

423 The culture medium for *E. coli* used in this study is based on $N^{-}C^{-}$ minimal
424 medium [54], containing K_2SO_4 (1 g), $K_2HPO_4 \cdot 3H_2O$ (17.7 g), KH_2PO_4 (4.7 g),
425 $MgSO_4 \cdot 7H_2O$ (0.1 g) and NaCl (2.5 g) per liter. The medium was supplemented
426 with 20 mM NH_4Cl, as nitrogen source, and 5 to 10 mM glycerol, as the sole carbon
427 source. *S. cerevisiae* were cultured in yeast nitrogen base medium (without amino
428 acids) and supplemented with 0.5% glucose. All chemicals were purchased from
429 Carl Roth, Karlsruhe, Germany. When needed, 0.1 mg/ml ampicillin (stock
430 prepared fresh and stored at -20ºC) and/or 0.067 mM methionine (stock stored
431 at 4ºC) were added to the culture

432

433 *Growth protocol for E. coli*

434 Cells were taken from a -80ºC glycerol stock, streaked out on a LB agar plate and
435 incubated around 12 hours at 37ºC. A single colony was picked and grown in batch
436 culture. For temperatures up to 39ºC, cells were grown first on LB at the desired
437 temperature (seed culture). Before reaching starvation, they were diluted and
438 inoculated into pre-warmed minimal medium supplemented with glycerol (pre-
439 culture). Cells grew in the pre-culture for several doublings to ensure exponential
440 growth and were then diluted and inoculated into pre-warmed glycerol minimal
441 medium (experimental culture). Inoculation into the latter was chosen such that
442 cells perform at least three additional doublings in the experimental culture
443 before growth was measured. For high temperatures (above 39ºC), the seed
444 culture medium used was glycerol minimal medium with 1% LB in order to help
445 the cells transition into the pre-culture.
446
447 For small culture volumes, 5 ml of culture were grown in 20 mm × 150 mm glass
448 test tubes (Fisher Scientific, Hampton, NH, USA) with disposable, polypropylene
449 Kim-Kap closures (Kimble Chase, Vineland, NJ, USA). Larger volumes, 25 ml, 50 ml
450 and 100 ml were grown in 125 ml, 250 ml and 500 ml baffled Erlenmeyer flasks
451 (Carl Roth, Karlsruhe, Germany), respectively, and Kim-Kap closures. All cultures
452 were grown in a shaking water bath (WSB-30, Witeg, Wertheim, Germany) with
453 water bath preservative (Akasolv, Akadia, Mannheim, Germany).
454
455 *Growth protocol for S. cerevisiae*
456 Cells were streaked from a -80ºC glycerol stock onto a YPD agar plate and
457 incubated for approximately 30 hours at 30ºC. A single colony was picked and
458 grown in batch culture with 4 mL NBM containing 1% YPD. Where necessary, the

459 culture was supplemented with methionine (0.067 mM). All cultures were
460 incubated in a shaking water bath with the culture tubes angled parallel to the
461 direction of shaking. The culture tubes and shaking water bath used were identical
462 to those used for the cultivation of *E. coli*.
463
464 *Protocol to induce long lag times at high temperatures*
465 Bacteria were first grown in minimal medium supplemented with glycerol as a
466 carbon substrate, as described above, at the desired temperature (37 to 45ºC).
467 After carbon depletion, cultures starved for 1 h to 24 h. Then, cultures were
468 diluted into fresh $N^{-}C^{-}$ supplemented with glycerol and NH_4Cl and allowed to
469 recover.
470
471 *Quantification of lag time*
472 The lag time after glycerol re-addition was extracted from optical density
473 measurements, and corrected for the loss of viability during the period of
474 starvation. Growth was modeled as $\mathrm{OD}_{600} = A + Be^{\mu t}$, which for long times
475 converges to $\lim_{t\to\infty} \mathrm{OD}_{600} = Be^{\mu t} = (A+B)e^{\mu(t-T_{\mathrm{lag}})}$, with lag time T_{lag}. We
476 extracted growth rate μ and the growing fraction of cells, B, from the time
477 derivative of optical density $\mathrm{d}\,\mathrm{OD}_{600}/\mathrm{d}t = \mu B e^{\mu t}$, using a least square fit across
478 the recovery regime where the time derivative increases exponentially. We
479 measure $(A+B)$ as the optical density after dilution. The lag time $T_{\mathrm{lag}} =$
480 $-\mu^{-1}\ln(B/(A+B))$, can then be calculated from the extracted parameters.
481 Lastly, because optical density measurements do not distinguish between living
482 and dead cells in the culture, and a fraction of the culture has perished during

483 starvation, we corrected the lag time estimation by subtracting the number of
484 dead cells N_d from the initial number $N(0) = A + B$. This gives a correction factor
485 $-\mu^{-1} \ln\left(\frac{N(0)}{N_\mathrm{d}}\right)$. For 5 h starvation at 45ºC, about one third of the cells perish. Thus,
486 with growth rate 0.45/h at 45ºC, this yields a correction factor of 0.9 h. In the main
487 text, all lag times are corrected for perished cells. Note that the bi-exponential fits
488 in Fig. 1, that include dynamics of both death and growth, are not used to extract
489 lag times.
490
491 *Time-lapse microscopy*
492 Microscopy was performed using agar pads in glass-bottom dishes. Agar pads
493 contained medium identical to the culture medium, $N^{-}C^{-}$ supplemented with 20
494 mM NH_4Cl, 20 mM Glycerol and 2 % low melting point agarose (Carl Roth,
495 Karlsruhe, Germany). Cells were diluted and pipetted on the prewarmed agar pad
496 and kept in the incubator. After the surface of the agar pad had dried, the agar pad
497 was flipped on the glass window of a prewarmed glass bottom dish. The glass
498 bottom dishes were sealed with parafilm to reduce evaporation.
499
500 Time-lapse microscopy was performed using a Nikon Ti-E microscope controlled
501 by NIS-Elements (Nikon, Tokyo, Japan). We used a phase contrast Plan Apo 100x
502 oil objective, with numerical aperture of 1.45 and a refractive index of 1.515
503 (Nikon, Tokyo, Japan) and a SCMOS camera (Zyla-5.5, Andor, Belfast, Northern
504 Ireland) with a binning of 1x1, a readout rate of 200 MHz and an exposure time of
505 200 ms. Conversion gain was set on 1/3 Dual gain and the spurious noise filter
506 was activated. The calibration from length units to pixels was defined as

507 0.07 μm/px. Measurements were performed with activated perfect focus system
508 and a PriorScan III drive stage. Temperature control was set by the Okolab Cage
509 Incubation System and confirmed with manual temperature measurements. Cell
510 growth was monitored for 24 hours with continuous acquisition of phase-contrast
511 and fluorescence images every 30 min at the desired temperature, e.g. 45ºC.
512
513 *Live/dead stain*
514 Commercial BacLight®LIVE/DEAD (Thermo Fisher Scientific Inc., Waltham,
515 Massachusetts, USA) staining was used when cells were microscopically imaged,
516 according to manufacturing specifications.
517
518 *Heat shock protocol*
519 Heat shocks were performed by transferring batch cultures (5 ml culture volume
520 in a 20 mm x 150 mm borosilicate glass tube (Fisher Scientific, NH, USA)) from
521 one water bath to another (WSB-30, Witeg, Wertheim, Germany). Water baths
522 were pre-set and equilibrated at the desired temperatures.
523
524 *Antibiotic treatment*
525 To measure survival upon antibiotic treatment, cells were first grown in minimal
526 medium with glycerol, as described above. A first sample of the culture was
527 extracted during exponential growth and supplemented with ampicillin, glycerol,
528 and with or without methionine. Viability was then measured over time by plate
529 counting, as described above.
530
531 *Survival quantification*

532 Survival in starvation was quantified by counting colony forming units (CFU).
533 Samples were diluted in carbon free $N^{-}C^{-}$ minimal medium and spread on LB
534 agar plates using Rattler Plating Beads (Zymo Research, Irvine, CA, USA) with a
535 target density of 200 colonies per plate. LB agar was supplemented with
536 25 μg/ml 2,3,5-triphenyltetrazolium chloride to stain colonies and increase
537 contrast for automated colony counting (Scan 1200, Interscience, Saint-Nom-la-
538 Bretèche, France). Staining or automation of counting had no significant effect on
539 viability measurements or accuracy, compared to unstained, manually counted
540 samples (<1% systematic error). Petri dishes were 92 x 16 mm (Sarstedt,
541 Nümbrecht, Germany) and agar plates were incubated for 12 hours at 37ºC to
542 ensure optimal colony size.
543
544 *Numerical analysis of the model*
545 The numerical solution in Fig. 3B was obtained by numerically integrating Eqs. (1-
546 3) using the nonstiff differential equation solver *ode45* in Matlab (Mathworks,
547 Natick, MA, USA). Initial conditions were $c_{\mathrm{met}}(0) = 0$ and $\phi_{\mathrm{MetA}}(0)$ ranging from
548 $2 \cdot 10^{-5}$ to $2 \cdot 10^{-4}$. The parameters used in the calculations were $a_1 =$
549 $4.06\ \mathrm{M}^{-1}, a_2 = 3.1 \cdot 10^{-5},\ a_3 = 148\ \mathrm{M}^{-2},\ \chi_{\mathrm{MetA}} = 2.79 \cdot 10^{-3},\ K_{\mathrm{M}} =$
550 10^{-6} M, see Table S2.
551
552 The phase diagrams in Fig. S4 were calculated by solving Eq. (S12) using the *solve*
553 function in Matlab (Mathworks, Natick, MA, USA). We shaded the regions
554 according to the number of stable fixed-points at concentrations higher or equal
555 to zero. One solution at $c^{*}_{\mathrm{met}} = 0$ (stable) was denoted 'non-growing region'. Two
556 zeros, $c^{*,1}_{\mathrm{met}} = 0$ (unstable) and $c^{*,2}_{\mathrm{met}} > 0$ (stable) was denoted 'growth region'.

557 Three zeros was denoted as the 'bistable region'. If methionine influx was
558 included, Fig. S4E, one stable solution at $c^*_{\mathrm{met}} > 0$ means that cells can grow on
559 external methionine. This region was shaded 'grey to white' to symbolize the
560 growth rate dependence on the methionine influx. The parameters used in the
561 calculations were $a_1 = 4.06\ \mathrm{M}^{-1}, a_2 = 3.1 \cdot 10^{-5}$, $a_3 = 148\ \mathrm{M}^{-2}$, $\chi_{\mathrm{MetA}} =$
562 $2.79 \cdot 10^{-3}$, $K_{\mathrm{M}} = 10^{-6}$ M, see Table S2.
563
564 *Statistical analysis*
565 Lag times with individual tests, e.g. methionine versus no methionine, were
566 performed in 2-3 biological repeats as mentioned in figure captions and are
567 reported with one standard deviation. Measurements that are quantitative tests,
568 e.g. influence of starvation time, were performed as single repeats, at multiple
569 different perturbation strength. Results of fits are reported with standard error.
570 Measurements of cell survival to antibiotic treatment were performed in
571 duplicates for each temperature. Survival measurements upon temperature shift
572 from 37, 40, 42 and 45 °C to 50ºC were performed at least twice for wild-type and
573 MetA stabilized mutants.
574
575

576 **REFERENCES**

577 1. Yura, T. & Nakahigashi, K. Regulation of the heat-shock response. *Current*
578 *Opinion in Microbiology* **2**, 153–158 (1999).
579 2. Arsène, F., Tomoyasu, T. & Bukau, B. The heat shock response of Escherichia
580 coli. *International Journal of Food Microbiology* **55**, 3–9 (2000).
581 3. Richter, K., Haslbeck, M. & Buchner, J. The Heat Shock Response: Life on the
582 Verge of Death. *Molecular Cell* **40**, 253–266 (2010).
583 4. Bukau, B. Regulation of the Escherichia coli heat-shock response. *Molecular*
584 *Microbiology* **9**, 671–680 (1993).
585 5. Laskowska, E., Kuczyńska-Wiśnik, D., Skórko-Glonek, J. & Taylor, A.
586 Degradation by proteases Lon, Clp and HtrA, of Escherichia coli proteins
587 aggregated in vivo by heat shock; HtrA protease action in vivo and in vitro.
588 *Molecular Microbiology* **22**, 555–571 (1996).
589 6. Nonaka, G., Blankschien, M., Herman, C., Gross, C. A. & Rhodius, V. A. Regulon
590 and promoter analysis of the E. coli heat-shock factor, σ32, reveals a
591 multifaceted cellular response to heat stress. *Genes Dev.* **20**, 1776–1789
592 (2006).
593 7. Marcén, M., Ruiz, V., Serrano, M. J., Condón, S. & Mañas, P. Oxidative stress in E.
594 coli cells upon exposure to heat treatments. *International Journal of Food*
595 *Microbiology* **241**, 198–205 (2017).
596 8. Mackey, B. M. & Seymour, D. A. The Effect of Catalase on Recovery of Heat-
597 injured DNA-repair Mutants of Escherichia coli. *Microbiology,* **133**, 1601–1610
598 (1987).
599 9. Privalle, C. T. & Fridovich, I. Induction of superoxide dismutase in Escherichia
600 coli by heat shock. *PNAS* **84**, 2723–2726 (1987).

601 10. Marcén, M., Cebrián, G., Ruiz-Artiga, V., Condón, S. & Mañas, P. Protective effect
602 of glutathione on Escherichia coli cells upon lethal heat stress. *Food Research*
603 *International* **121**, 806–811 (2019).
604 11. Oliver, J. D. Recent findings on the viable but nonculturable state in pathogenic
605 bacteria. *FEMS Microbiol Rev* **34**, 415–425 (2010).
606 12. Xu, H.-S. *et al.* Survival and viability of nonculturableEscherichia coli andVibrio
607 cholerae in the estuarine and marine environment. *Microb Ecol* **8**, 313–323
608 (1982).
609 13. Oliver, J. D. The viable but nonculturable state in bacteria. *J. Microbiol.* **43 Spec**
610 **No**, 93–100 (2005).
611 14. Balaban, N. Q., Merrin, J., Chait, R., Kowalik, L. & Leibler, S. Bacterial Persistence
612 as a Phenotypic Switch. *Science* **305**, 1622–1625 (2004).
613 15. Balaban, N. Q. *et al.* Definitions and guidelines for research on antibiotic
614 persistence. *Nature Reviews Microbiology* **17**, 441–448 (2019).
615 16. Li, L., Mendis, N., Trigui, H., Oliver, J. D. & Faucher, S. P. The importance of the
616 viable but non-culturable state in human bacterial pathogens. *Front. Microbiol.*
617 **5**, (2014).
618 17. Zhao, X., Zhong, J., Wei, C., Lin, C.-W. & Ding, T. Current Perspectives on Viable
619 but Non-culturable State in Foodborne Pathogens. *Front. Microbiol.* **8**, (2017).
620 18. Pinto, D., Santos, M. A. & Chambel, L. Thirty years of viable but nonculturable
621 state research: Unsolved molecular mechanisms. *Critical Reviews in*
622 *Microbiology* **41**, 61–76 (2015).
623 19. Harms, A., Maisonneuve, E. & Gerdes, K. Mechanisms of bacterial persistence
624 during stress and antibiotic exposure. *Science* **354**, aaf4268 (2016).

625 20. Laman Trip, D. S. & Youk, H. Yeasts collectively extend the limits of habitable
626 temperatures by secreting glutathione. *Nature Microbiology* **5**, 943–954
627 (2020).
628 21. Dill, K. A., Ghosh, K. & Schmit, J. D. Physical limits of cells and proteomes.
629 *Proceedings of the National Academy of Sciences* **108**, 17876–17882 (2011).
630 22. Leuenberger, P. *et al.* Cell-wide analysis of protein thermal unfolding reveals
631 determinants of thermostability. *Science* **355**, eaai7825 (2017).
632 23. Ron, E. Z. & Davis, B. D. Growth Rate of Escherichia coli at Elevated
633 Temperatures: Limitation by Methionine. *J Bacteriol* **107**, 391–396 (1971).
634 24. Biran, D., Brot, N., Weissbach, H. & Ron, E. Z. Heat shock-dependent
635 transcriptional activation of the metA gene of Escherichia coli. *Journal of*
636 *bacteriology* **177**, 1374–1379 (1995).
637 25. Biran, D., Gur, E., Gollan, L. & Ron, E. Z. Control of methionine biosynthesis in
638 Escherichia coli by proteolysis. *Molecular Microbiology* **37**, 1436–1443 (2000).
639 26. Gur, E., Biran, D., Gazit, E. & Ron, E. Z. In vivo aggregation of a single enzyme
640 limits growth of Escherichia coli at elevated temperatures. *Molecular*
641 *Microbiology* **46**, 1391–1397 (2002).
642 27. Mordukhova, E. A., Kim, D. & Pan, J.-G. Stabilized homoserine o-
643 succinyltransferases (MetA) or L-methionine partially recovers the growth
644 defect in Escherichia coli lacking ATP-dependent proteases or the DnaK
645 chaperone. *BMC Microbiol* **13**, 179 (2013).
646 28. Jung, I. L. & Kim, I. G. Polyamines and Glutamate Decarboxylase-based Acid
647 Resistance in *Escherichia coli*. *J. Biol. Chem.* **278**, 22846–22852 (2003).
648 29. Khan, A. U., Di Mascio, P., Medeiros, M. H. & Wilson, T. Spermine and
649 spermidine protection of plasmid DNA against single-strand breaks induced

650 by singlet oxygen. *Proceedings of the National Academy of Sciences* **89**, 11428–
651 11430 (1992).
652 30. Shah, P. & Swiatlo, E. A multifaceted role for polyamines in bacterial
653 pathogens. *Molecular Microbiology* **68**, 4–16 (2008).
654 31. Strogatz, S. H. *Nonlinear dynamics and chaos with student solutions manual:*
655 *With applications to physics, biology, chemistry, and engineering*. (CRC press,
656 2018).
657 32. Friedman, N., Cai, L. & Xie, X. S. Linking Stochastic Dynamics to Population
658 Distribution: An Analytical Framework of Gene Expression. *Phys. Rev. Lett.* **97**,
659 168302 (2006).
660 33. Taniguchi, Y. *et al.* Quantifying E. coli Proteome and Transcriptome with
661 Single-Molecule Sensitivity in Single Cells. *Science* **329**, 533–538 (2010).
662 34. Nierhaus, D. & Nierhaus, K. H. Identification of the Chloramphenicol-Binding
663 Protein in Escherichia coli Ribosomes by Partial Reconstitution. *PNAS* **70**,
664 2224–2228 (1973).
665 35. Davidson, J. F., Whyte, B., Bissinger, P. H. & Schiestl, R. H. Oxidative stress is
666 involved in heat-induced cell death in Saccharomyces cerevisiae. *PNAS* **93**,
667 5116–5121 (1996).
668 36. Davidson, J. F. & Schiestl, R. H. Cytotoxic and Genotoxic Consequences of Heat
669 Stress Are Dependent on the Presence of Oxygen in Saccharomyces cerevisiae.
670 *Journal of Bacteriology* **183**, 4580–4587 (2001).
671 37. Lushchak, V. I. & Bagnyukova, T. V. Temperature increase results in oxidative
672 stress in goldfish tissues. 1. Indices of oxidative stress. *Comparative*
673 *Biochemistry and Physiology Part C: Toxicology & Pharmacology* **143**, 30–35
674 (2006).

675 38. Lushchak, V. I. & Bagnyukova, T. V. Temperature increase results in oxidative
676 stress in goldfish tissues. 2. Antioxidant and associated enzymes. *Comparative*
677 *Biochemistry and Physiology Part C: Toxicology & Pharmacology* **143**, 36–41
678 (2006).
679 39. Murata, M. *et al.* Molecular Strategy for Survival at a Critical High Temperature
680 in Eschierichia coli. *PLOS ONE* **6**, e20063 (2011).
681 40. Mirzaei, H. & Regnier, F. Protein:protein aggregation induced by protein
682 oxidation. *Journal of Chromatography B* **873**, 8–14 (2008).
683 41. Lévy, E. *et al.* Causative Links between Protein Aggregation and Oxidative
684 Stress: A Review. *International Journal of Molecular Sciences* **20**, 3896 (2019).
685 42. Davies, K. J. A. & Lin, S. W. Degradation of oxidatively denatured proteins in
686 Escherichia coli. *Free Radical Biology and Medicine* **5**, 215–223 (1988).
687 43. Pacifici, R. E. & Davies, K. J. A. Protein degradation as an index of oxidative
688 stress. in *Methods in Enzymology* vol. 186 485–502 (Academic Press, 1990).
689 44. Potrykus, K. & Cashel, M. (p)ppGpp: Still Magical? *Annual Review of*
690 *Microbiology* **62**, 35–51 (2008).
691 45. Lemke, J. J. *et al.* Direct regulation of Escherichia coli ribosomal protein
692 promoters by the transcription factors ppGpp and DksA. *PNAS* **108**, 5712–
693 5717 (2011).
694 46. Dalebroux, Z. D. & Swanson, M. S. ppGpp: magic beyond RNA polymerase. *Nat*
695 *Rev Microbiol* **10**, 203–212 (2012).
696 47. Schreiber, G., Ron, E. Z. & Glaser, G. ppGpp-mediated regulation of DNA
697 replication and cell division in Escherichia coli. *Current Microbiology* **30**, 27–
698 32 (1995).

699 48. Wang, J. D., Sanders, G. M. & Grossman, A. D. Nutritional Control of Elongation
700 of DNA Replication by (p)ppGpp. *Cell* **128**, 865–875 (2007).
701 49. Gottesman, S. & Maurizi, M. R. Regulation by proteolysis: energy-dependent
702 proteases and their targets. *Microbiology and Molecular Biology Reviews* **56**,
703 592–621 (1992).
704 50. Gardner, A., West, S. A. & Griffin, A. S. Is Bacterial Persistence a Social Trait?
705 *PLoS ONE* **2**, e752 (2007).
706 51. Veening, J.-W., Smits, W. K. & Kuipers, O. P. Bistability, Epigenetics, and Bet-
707 Hedging in Bacteria. *Annual Review of Microbiology* **62**, 193–210 (2008).
708 52. Verstraeten, N. *et al.* Obg and Membrane Depolarization Are Part of a Microbial
709 Bet-Hedging Strategy that Leads to Antibiotic Tolerance. *Molecular Cell* **59**, 9–
710 21 (2015).
711 53. Soupene, E. *et al.* Physiological Studies of Escherichia coli Strain MG1655:
712 Growth Defects and Apparent Cross-Regulation of Gene Expression. *J Bacteriol*
713 **185**, 5611–5626 (2003).
714 54. Csonka, L. N., Ikeda, T. P., Fletcher, S. A. & Kustu, S. The accumulation of
715 glutamate is necessary for optimal growth of Salmonella typhimurium in
716 media of high osmolality but not induction of the proU operon. *Journal of*
717 *Bacteriology* **176**, 6324–6333 (1994).
718
719